

Quasiharmonic analysis of protein energy landscapes from pressure-temperature molecular dynamics simulations

Jocelyn M. Rodgers,¹ Russell J. Hemley,² and Toshiko Ichiye^{1,a)}

¹Department of Chemistry, Georgetown University, Washington, DC 20057, USA

²Department of Civil and Environmental Engineering, The George Washington University, Washington, DC 20052, USA

(Received 28 April 2017; accepted 7 September 2017; published online 27 September 2017)

Positional fluctuations of an atom in a protein can be described as motion in an effective local energy minimum created by the surrounding protein atoms. The dependence of atomic fluctuations on both temperature (T) and pressure (P) has been used to probe the nature of these minima, which are generally described as harmonic in experiments such as x-ray crystallography and neutron scattering. Here, a quasiharmonic analysis method is presented in which the P - T dependence of atomic fluctuations is in terms of an intrinsic isobaric thermal expansivity α_P and an intrinsic isothermal compressibility κ_T . The method is tested on previously reported mean-square displacements from P - T molecular dynamics simulations of lysozyme, which were interpreted to have a pressure-independent dynamical transition T_g near 200 K and a change in the pressure dependence near 480 MPa. Our quasiharmonic analysis of the same data shows that the P - T dependence can be described in terms of α_P and κ_T where below T_g , the temperature dependence is frozen at the T_g value. In addition, the purported transition at 480 MPa is reinterpreted as a consequence of the pressure dependence of T_g and the quasiharmonic frequencies. The former also indicates that barrier heights between substates are pressure dependent in these data. Furthermore, the insights gained from this quasiharmonic analysis, which was of the energy landscape near the native state of a protein, suggest that similar analyses of other simulations may be useful in understanding such phenomena as pressure-induced protein unfolding. *Published by AIP Publishing.* <https://doi.org/10.1063/1.5003823>

I. INTRODUCTION

The concept of an energy landscape has been useful in describing a variety of phenomena in proteins, including protein function and folding.^{1,2} The structure of a folded protein from an X-ray crystallographic or nuclear magnetic resonance (NMR) solution structure determination can be considered to be a minimum in this rough landscape. Conformational transitions from this minimum to other local minima may occur: nearby conformations may correspond to states important for protein function, while farther ones may correspond to folding intermediates. The landscape has often been explored by using temperature variations of the system,³ which vary the thermal energy and the system volume via thermal expansivity. More recently, variations in pressure have also been used,^{4,5} which affects only the system volume via the compressibility. Pressure could change the shape or depth of minima or the distance or barriers between minima.

While the energy landscape is a multidimensional potential energy surface dependent on the coordinates of all atoms in the system, another useful concept is the local effective potential energy minimum in which a given atom fluctuates. In a given conformational state, the potential energy well is created by the neighboring atoms and can be characterized by the

average position of the atom in that state and the mean-square fluctuations about that position. For instance, the temperature factors used in X-ray crystallographic refinement of structures arise in part from thermal fluctuations about an average position and thus can assess the width of the minimum. In addition, the mean-square displacements from neutron scattering studies can also be related to the mean-square fluctuations. In proteins, this local energy minimum is generally assumed to be an isotropic harmonic three-dimensional well although anisotropic and even anharmonic wells can be considered. In fact, an increasing number of protein structures in the Protein Data Bank⁶ (PDB) report anisotropic temperature factors.

The potential energy surface corresponding to a given conformational state of a protein is rough, with multiple local minima corresponding to many substates within the conformational state. Most atoms can be considered to fluctuate in a single energy minimum on a short enough time scale, although sometimes transitions to other local minima may occur via processes such as dihedral angle transitions.^{7,8} On longer time scales, the motions of a given atom couple to an increasing number of atoms, resulting in “collective motions”⁹ that can be considered as phonons in a normal mode approximation. Interestingly, the frequency distribution demonstrates a quadratic Debye behavior characteristic of acoustic phonons even at wavelengths significantly smaller than the size of the protein (i.e., time scales as low as ~ 1 ps), apparently because

^{a)}E-mail: toshiko.ichiye@georgetown.edu

the protein and solvent behave as a continuum due to the similarities in the weak interactions within the protein and between the protein and solvent.³ On longer time scales, these collective motions can also give rise to transitions to other substates. Interestingly, a dynamical transition has been observed in atomic fluctuations of protein atoms at a transition temperature $T_g \sim 200$ K, which has been likened to the glass transition of the protein.^{10–12} Below T_g , the interpretation is that thermal energy is insufficient to make transitions so atoms get trapped in a single substate, which corresponds to an underlying potential energy minimum. On the other hand, above T_g , the interpretation is that thermal fluctuations cause transitions between different substates within the same conformational state. However, proteins are not typical glass-forming systems and thus do not necessarily follow typical glass behavior. In fact, a perhaps non-intuitive behavior of proteins is that they unfold at high pressure. This has been explained as the result of hydration of the interior of the protein, which results in a lower system volume since water molecules can fill voids in the folded protein.

To describe more complex motion, at least two types of deviation from strictly harmonic behavior can be considered.^{13,14} In a quasiharmonic approximation, individual atoms are considered to move in harmonic potentials but expansion or contraction of the system due to pressure or temperature changes are accounted for since they change the available space for a given atom created by its neighbors. Thus, the frequencies vary with volume, an approach used extensively for problems in condensed matter and materials physics.^{13,14} In a full anharmonic treatment, individual atoms are considered to move within energy basins that are anharmonic in shape, which leads to additional frequency changes with temperature than expected from volume changes alone. Thus, the frequencies are dependent on both volume and temperature. In the case of solids, the anharmonic contributions arise from complex phonon-phonon interactions.¹⁵ On the other hand, the total anharmonic contribution at a given pressure and temperature can be determined experimentally from appropriate measurements and thermodynamic relations.¹³

The approach of understanding how volume changes affect the frequencies apparently has not yet been applied to understanding the vibrational dynamics of biological molecules. Such a treatment may be useful because the complex dynamics of proteins described above even in one conformation state demonstrates the breakdown of a simple harmonic description of behavior of the component atoms. For instance, the nonlinear temperature dependence of the temperature factors above T_g ¹² and comparisons of quasiharmonic modes calculated from molecular dynamics simulations at room temperature with those from normal modes analysis⁹ suggest that the force constants are changing with temperature. In addition, the protein dynamical transition has been attributed to solvent-driven activation of anharmonic dynamics above T_g ^{16,17} and the observation of transitional behavior of positional distributions from protein simulations at room temperature shows that the fluctuations can be considerably anharmonic.⁷ In particular, since transitions between substates appear to occur above T_g , which should increase the

volume, a quasiharmonic approximation appears warranted for understanding the effects of temperature and pressure on fluctuations.

Examining atomic fluctuations in molecular dynamics simulations of biological macromolecules under pressure can provide information about their energy landscape. For example, Meinhold *et al.*⁵ used both pressure and temperature to explore the energy landscape of hen egg white lysozyme (HEWL) in water using molecular dynamics (MD) simulations at pressures between 0.1 and 1000 MPa and at temperatures from 20 to 320 K. Experimentally, HEWL reversibly denatures above 350 MPa or below 260 K on the hour time scale to an unfolded state that appears to be quite different from high temperature or chemical denaturant unfolded states.¹⁸ However, since the simulations were heated, pressurized, and equilibrated from the energy minimized NMR structure in less than 1 ns and the total length of each simulation was 1 ns, none of the simulations can be expected to be in the thermodynamically favored state. Instead, they probe the energy landscape near the native state. In these studies, the reported data are the time-dependent mean-square displacements $d^2(\tau)$ of hydrogen atoms, which were chosen in part because they can be measured directly in neutron scattering experiments. Meinhold *et al.*⁵ have shown that the dynamics of protein hydrogen atoms are a good measure of the dynamics of all protein atoms. $d^2(\tau = 1 \text{ ps})_P$ increased linearly with temperature below $T_g \approx 200$ K and nonlinearly at a higher rate above T_g , which was ascribed to the protein dynamical transition. Since T_g appeared to be independent of pressure, they concluded that the barrier height between potential energy minima was independent of pressure. In addition, an effective environmental force constant, k_{eff} , for the underlying harmonic potential was obtained from $d^2(\tau = 1 \text{ ps})|_{T_g}$ from the linear regime below T_g . Interestingly, k_{eff} was found to increase linearly with pressure below 480 MPa and linearly but at a slower rate above 480 MPa, which was attributed to a qualitative change in the pressure response of the protein energy landscape.

Here, a method for analyzing atomic fluctuations in macromolecules is presented, which utilizes the quasiharmonic approximation in which the underlying modes are assumed to have frequencies that vary with volume. The approach is suited for macromolecules with rough potential energy landscapes with regions corresponding to defined conformational states, such as proteins. Assuming that each atom of the protein moves in a local effective potential created by its neighboring atoms, the protein is described as a classical Einstein-type model of a solid where the atoms are independent harmonic oscillators with identical quasiharmonic frequencies. The temperature and pressure dependence of the average atomic fluctuations of the protein are thus described in terms of an intrinsic isobaric thermal expansivity α_P and an intrinsic isothermal compressibility κ_T , respectively. These are intrinsic properties of the protein, independent of direct solvent effects. To illustrate the applicability and utility of this approach, the HEWL simulation data from Meinhold *et al.*⁵ are reexamined using our quasiharmonic analysis. Although the analysis of mean-square fluctuations of protein heavy atoms would be ideal, Meinhold *et al.*⁵ report only mean-square

displacements of hydrogen atoms, which are shown to be a good measure of the dynamics of all protein atoms. The approach leads to reassessment of the prior conclusions, namely, pressure independent barrier heights between local minima and a transition in the pressure response of the energy surface. Notably, we find the purported transition at 480 MPa can be interpreted as a consequence of the pressure dependences of T_g and of the quasiharmonic frequencies. The former also indicates that barrier heights between local minima are pressure dependent. More broadly, this type of quasiharmonic analysis of computer simulation of proteins may be useful in understanding phenomena such as pressure-induced protein unfolding. Although more proteins need to be examined, the results here suggest that while pressure might be expected to reduce fluctuations by compressive effects on a single substate, it may also favor transitions to other substates and thus enhance fluctuations. Since these other substates can include more solvated conformations, these transitions may ultimately lead to unfolding.

II. THEORETICAL METHODS

A. Quasiharmonicity and anharmonicity

Deviations from a purely harmonic system with a force constant k and volume and temperature independent frequencies can be described as quasiharmonic or anharmonic. Formally, a quasiharmonic system has vibrational frequencies that vary only because the effective available space changes as the material expands or contracts with pressure and/or temperature¹⁴ so that frequencies vary directly only with volume. In addition, an anharmonic system has vibrational frequencies that are dependent on both volume and temperature.¹⁴

Generally, a potential energy minimum can be described by a volume and temperature dependent effective force constant $k(V, T)$ defined as

$$dk(V, T) = \left(\frac{\partial k}{\partial V}\right)_T dV + \left(\frac{\partial k}{\partial T}\right)_V dT \quad (1)$$

or, in terms of pressures and temperatures, as

$$dk(P, T) = \left(\frac{\partial k}{\partial P}\right)_T dP + \left(\frac{\partial k}{\partial T}\right)_P dT, \quad (2)$$

where

$$\left(\frac{\partial k}{\partial P}\right)_T = \left(\frac{\partial k}{\partial V}\right)_T \left(\frac{\partial V}{\partial P}\right)_T, \quad (3)$$

$$\left(\frac{\partial k}{\partial T}\right)_P = \left(\frac{\partial k}{\partial V}\right)_T \left(\frac{\partial V}{\partial T}\right)_P + \left(\frac{\partial k}{\partial T}\right)_V. \quad (4)$$

In Eqs. (3) and (4), a harmonic system has $(\partial k/\partial P)_T = (\partial k/\partial T)_P = 0$, a quasiharmonic system has $(\partial k/\partial T)_V = 0$ so that $k(P, T) = k(V(P, T))$, and an anharmonic system has all non-zero terms. Substituting Eqs. (3) and (4) into Eq. (2), the

quasiharmonic approximation can be written as

$$dk(P, T) = \left(\frac{\partial k}{\partial V}\right)_T \left(\frac{\partial V}{\partial P}\right)_T dP + \left(\frac{\partial k}{\partial V}\right)_T \left(\frac{\partial V}{\partial T}\right)_P dT. \quad (5)$$

The quantities in Eq. (5) can be identified with various thermodynamic parameters. For instance, the isothermal compressibility is

$$\kappa_T = -V^{-1}(\partial V/\partial P)_T \quad (6)$$

and the isobaric thermal expansivity is

$$\alpha_T = V^{-1}(\partial V/\partial P)_P. \quad (7)$$

The volume dependence of these quantities can be determined with respect to a reference pressure P_0 and a reference temperature T_0 , and Δ denotes differences with respect to reference quantities. The dependence of κ_T on V can be described as

$$\kappa_T = \kappa_{T,0} \left(\frac{V(P)}{V(P_0)}\right)^\mu, \quad (8)$$

where $\kappa_{T,0} = \kappa_T(P_0)$ and μ is a non-linearity index. Inserting this into Eq. (6) and integrating, one obtains the Moelwyn-Hughes isotherm¹⁹

$$\frac{V(P)}{V(P_0)} = (1 + \mu\kappa_{T,0}\Delta P)^{-1/\mu} \quad \mu \neq 0. \quad (9)$$

Similarly, the dependence of α_P on V can be described as

$$\alpha_P = \alpha_{P,0} \left(\frac{V(T)}{V(T_0)}\right)^\nu, \quad (10)$$

where $\alpha_{P,0} = \alpha_P(T_0)$ and ν is another non-linearity index. Inserting this into Eq. (7) and integrating, one obtains

$$\frac{V(T)}{V(T_0)} = \begin{cases} \exp(\alpha_{P,0}\Delta T) & \nu = 0 \\ (1 - \nu\alpha_{P,0}\Delta T)^{-1/\nu} & \nu \neq 0 \end{cases}. \quad (11)$$

[Note that since the fits here are over a very small range of temperatures, the case of a volume independent α_P such that $\nu = 0$ is explicitly considered in Eq. (11).]

The volume dependence of the force constant can be determined assuming that the effective force constant gives rise to phonon modes with frequency ω . Recognizing that $\omega^2 \propto k$,

$$\frac{V}{k} \left(\frac{\partial k}{\partial V}\right)_T = -2\gamma_T, \quad (12)$$

where γ_T is the Grüneisen parameter.¹⁴ In addition, the Grüneisen parameter is related to the non-linearity index μ for a Debye solid (which also holds for an Einstein solid) by²⁰

$$2\gamma_T = \mu - \frac{1}{3}. \quad (13)$$

Next, substituting Eqs. (9)–(12) into Eq. (5) and integrating leads to

$$k(P, T) = \begin{cases} k_0 [\exp(-\alpha_{P,0}\Delta T)(1 + \mu\kappa_{T,0}\Delta P)^{1/\mu}]^{(\mu - \frac{1}{3})} & \nu = 0, \quad \mu \neq 0 \\ k_0 [(1 - \nu\alpha_{P,0}\Delta T)^{1/\nu}(1 + \mu\kappa_{T,0}\Delta P)^{1/\mu}]^{(\mu - \frac{1}{3})} & \nu \neq 0, \quad \mu \neq 0 \end{cases}, \quad (14)$$

where $k_0 = k(P_0, T_0)$. Furthermore, if κ_T is assumed to be independent of T , $\kappa_{T,0} = \kappa_T(P_0, T_0)$ and if α_P is assumed independent of P , $\alpha_{P,0} = \alpha_P(P_0, T_0)$.

B. Mean-square displacements

The most direct measure of the effective local potential from a simulation would be the mean-square atomic fluctuations averaged over all protein atoms. However, the quantity calculated from the simulations by Meinhold *et al.*⁵ is $d^2(\tau) = \overline{\langle [\mathbf{r}_i(t) - \mathbf{r}_i(t + \tau)]^2 \rangle}$, where $\mathbf{r}_i(t)$ is the coordinate vector of atom i at time t , the angle brackets and over bar are the time and ensemble averages, respectively, of the hydrogen atoms, and $\tau = 1$ ps.

Assuming that each hydrogen atom can be considered to be in an effective local harmonic potential subject to Brownian fluctuations, the mean-square displacement can be related to the mean-square fluctuations $\sigma^2 = \overline{\langle \mathbf{r}_i(t)^2 \rangle}$ in the effective harmonic potential. In particular, assuming the energy minimum has a spring constant $M\omega_0^2$ and γ is the damping coefficient,

$$\begin{aligned} d^2(\tau) &= \overline{\langle \mathbf{r}_k(t)^2 \rangle} - 2\overline{\langle \mathbf{r}_k(t) \cdot \mathbf{r}_k(t + \tau) \rangle} + \overline{\langle \mathbf{r}_k(t + \tau)^2 \rangle} \\ &= 2\sigma^2 \left[1 - \exp(-\gamma\tau/2) \left(\cos(\omega_1\tau) + \frac{\gamma}{2\omega_1} \sin(\omega_1\tau) \right) \right], \end{aligned} \quad (15)$$

where $\omega_1^2 = \omega_0^2 + \gamma^2/4$. For the case studied in Meinhold *et al.*,⁵ the factor in large parenthesis in the second equality averages to zero since the mean-square displacement is averaged over all hydrogen atoms in the protein, which each have a different phase shift, and the exponential factor is constant. Thus, the reported $d^2(\tau) \rightarrow 2\sigma^2 = 6k_B T/k$, where k is the average local effective harmonic force constant for a hydrogen atom in the protein on a time scale τ so that only motions with time scales up to τ can contribute to the local effective harmonic potential. A slight increase in $d^2(\tau)$ for the hydrogen atoms in a protein has been noted between $\tau = 1$ ps and $\tau = 10$ ps for hydrogens;⁴ however, it was concluded that the 1 ps time scale is sufficient for probing the energy landscape near the NMR structure.

C. Fitting procedures

The data used for testing this quasiharmonic analysis are taken from the MD simulations of HEWL found in the work of Meinhold *et al.*,⁵ which gives details of the simulation methods and are repeated in the [supplementary material](#). Briefly, the simulations were performed using the Gromacs suite of programs^{21,22} with the all-atom OPLS-AA/L force field.²³

The initial structure was 1GXV²⁴ from the PDB,⁶ which was solved at 1 atm by NMR. The system was energy minimized, subsequently heated for 100 ps, and then pressurized and equilibrated for 600 ps using the extended-ensemble Nosé-Hoover/Parrinello-Rahman algorithms.^{25–28} The production phase of each temperature-pressure value was 1 ns and coordinates were saved at 0.1 ps for analysis. $d^2(1 \text{ ps})$ are reported for $0.1 \text{ MPa} \leq P \leq 1000 \text{ MPa}$ in 50 MPa intervals and $240 \text{ K} \leq T \leq 320 \text{ K}$ in 20 K intervals, which will be referred to as the “pressure” set, and for $0 \text{ K} < T \leq 320 \text{ K}$ in 20 K intervals and $P = 0.1, 300, 700, \text{ and } 1000 \text{ MPa}$, which will be referred to as the “temperature” set. In addition, k was reported for $0.1 \text{ MPa} \leq P \leq 1000 \text{ MPa}$ in 50 MPa intervals. To account for differences in the definition of k as well as significant figures of constants, their data for k were scaled accordingly using slopes of d^2 from the temperature set. The fits were performed using gnuplot. The goodness of fits for the parameters were examined via the reduced χ^2 , which is the mean-square residuals from the fit against the MD simulation data divided by the number of degrees of freedom, so that fits using different numbers of parameters can be compared.

III. RESULTS

The accuracy and utility of the quasiharmonic analysis are tested here by reexamining the MD simulation data for HEWL in the work of Meinhold *et al.*⁵ The reference state is chosen here as $P_0 = 0.1 \text{ MPa}$ and $T_0 = 298 \text{ K}$, although results appear independent of the choice of reference state. Under the assumption that the “glass” transition involves a smooth (non-discontinuous) transition, the high temperature data (well above where the glass transition temperature for proteins is typically found, i.e., $T \gg 200 \text{ K}$) are first fit assuming a pressure and temperature dependent k and then the low temperature data (i.e., $T \ll 200 \text{ K}$) are fit assuming that k is fixed to its value at (P, T_g) by varying T_g .

A. Above the “glass” transition

Above the “glass” transition temperature, the local atomic fluctuations of the protein are assumed to be close enough to harmonic so that any anharmonicity may be treated via a quasiharmonic approximation. In other words, the potential energy wells have force constants that are pressure and temperature dependent only via volumetric effects so are given by Eq. (14) in terms of a temperature-independent κ_T and a pressure-independent α_P , respectively. Substituting Eq. (14) into Eq. (15), the mean-square displacement $d^2(P, T)$ is given by

$$d^2(P, T) = \begin{cases} d_0^2 \frac{T}{T_0} \left[\exp(-\alpha_{P,0} \Delta T) (1 + \mu \kappa_{T,0} \Delta P)^{1/\mu} \right]^{\left(\frac{1}{3} - \mu\right)} & \nu = 0, \mu \neq 0 \\ d_0^2 \frac{T}{T_0} \left[(1 - \nu \alpha_{P,0} \Delta T)^{1/\nu} (1 + \mu \kappa_{T,0} \Delta P)^{1/\mu} \right]^{\left(\frac{1}{3} - \mu\right)} & \nu \neq 0, \mu \neq 0 \end{cases}, \quad (16)$$

TABLE I. Fit of $d^2(P, T)$ to MD simulation data. In both cases, $\nu = 0$.

μ	Constant	Fit value	Uncertainty	$\chi^2 \times 10^5$
0.70 ± 0.10	d_0^2 (\AA^2)	0.494 6	0.002 0	}3.26
	$\alpha_{P,0}$ (K^{-1})	0.011 25	0.002 9	
	$\kappa_{T,0}$ (MPa^{-1})	0.001 62	0.000 5	
1	d_0^2 (\AA^2)	0.492 4	0.001 5	}3.32
	$\alpha_{P,0}$ (K^{-1})	0.006 24	0.000 09	
	$\kappa_{T,0}$ (MPa^{-1})	0.000 82	0.000 01	

where $d_0^2 = d^2(P_0, T_0)$. The fits in this section utilize the pressure data set (i.e., $0.1 \text{ MPa} \leq P \leq 1000 \text{ MPa}$ at $240 \text{ K} \leq T \leq 320 \text{ K}$) from the HEWL MD simulation.

First, $d^2(P, T)$ calculated using Eq. (16) is fit to the MD pressure data to find d_0^2 , $\alpha_{P,0}$, $\kappa_{T,0}$, μ , and ν assuming $\nu \neq 0$ (Table S1 of the [supplementary material](#)). Since ν is very small with a very large uncertainty ($\nu = -0.004 \pm 0.104$), $d^2(P, T)$ is also fit to find d_0^2 , $\alpha_{P,0}$, $\kappa_{T,0}$, and μ assuming $\nu = 0$ (Table I and Table S2 of the [supplementary material](#)). Next, since μ was found to be close to 1 (i.e., $\mu = 0.70 \pm 0.10$), the ideal gas value, $d^2(P, T)$, calculated using Eq. (18) with $\mu = 1$ is fit to the MD pressure data to find d_0^2 , $\alpha_{P,0}$, $\kappa_{T,0}$, and ν assuming $\nu \neq 0$ (Table S3 of the [supplementary material](#)). Since ν is still small ($\nu = -0.01 \pm 0.19$), over the small temperature range examined here, α_P appears independent of the volume [$\nu = 0$ in Eq. (9)], although it is likely to depend on the volume over a larger temperature range. Thus, $d^2(P, T)$ is fit for d_0^2 , $\alpha_{P,0}$, and $\kappa_{T,0}$ assuming $\mu = 1$ and $\nu = 0$ (Table I and Table S4 of the [supplementary material](#)). The above-mentioned results all show good agreement with the simulation data and differences between fitting μ or ν and holding them fixed are barely visible to the eye so figures in the remainder of the main text are for the $\mu = 0.7$ and $\nu = 0$ case. In particular, $d^2(P, T)$ versus pressure P at various temperatures shows good agreement with the simulation data (Fig. 1).

B. Below the glass transition

Although $d^2(P, T)$ calculated from Eq. (16) using parameters fit to the pressure data set, which contains data only at high temperatures, reproduce the high temperature region, they do not reproduce the low temperature region (i.e., Fig. S1 of the [supplementary material](#)). The most likely cause is the onset of glassy behavior. Here, the protein is assumed to exhibit glassy behavior in the low temperature region as in Meinhold *et al.*⁵ so that the thermal fluctuations are assumed to no longer cause transitions to other substates that lead to volume changes while pressure still causes volume changes. Thus, the volume below T_g at constant P is frozen at its T_g value but still is dependent on P with the same values of the parameters as above T_g and the magnitude of k at a given P becomes frozen at T_g . In other words, below the ‘‘glass’’ transition temperature, the local atomic fluctuations of the protein are assumed to be

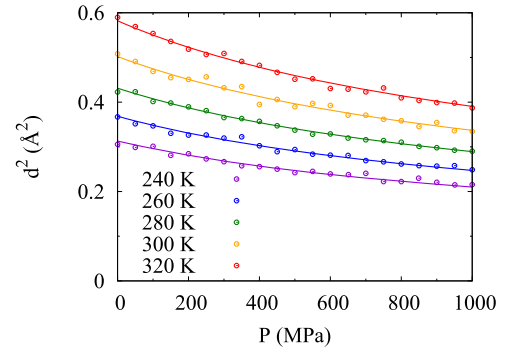


FIG. 1. Fit of mean-square displacements $d^2(P, T)$ versus pressure P at various temperatures calculated with $\mu = 0.7$ and $\nu = 0$ using parameters in Table I compared to MD simulation data.

quasiharmonic with force constants that have a different value at each pressure but are independent of temperature but continuous at T_g with the high temperature values.

An important question in general is the possible pressure dependence of T_g , reminiscent of the question of the pressure dependence of T_g in glass forming materials.²⁹ Meinhold *et al.*⁵ concluded from examining their data that T_g was independent of pressure. However, our approach identifies the pressure, temperature, and volumes dependences of T_g . For instance, if T_g is assumed to be independent of pressure, then

$$T_g(P) = T_{g,0}. \quad (17)$$

The pressure dependence of T_g can also be simply described by a linear equation

$$T_g(P) = T_{g,0} - c\Delta P, \quad (18)$$

where $T_{g,0}$ is T_g at the reference pressure and c is a constant. Alternatively, if the volume at P relative to volume at the reference pressure is given by Eq. (9), T_g at P can be assumed to occur at the same volume change relative to T_g at the reference pressure, which is given by Eq. (11). Assuming $\nu = 0$ as indicated by the results in Sec. III A, this implies that T_g is logarithmically dependent on pressure according to

$$T_g(P) = T_{g,0} - \frac{1}{c\alpha_{P,0}} \ln(1 + c\kappa_{T,0}\Delta P), \quad (19)$$

where again $T_{g,0}$ is T_g at the reference pressure and c is a constant. Since the physical origin of $\alpha_{P,0}$ appears to be different from that of $\kappa_{T,0}$ as discussed in Sec. IV, the volume change associated with pressure that gives rise to changes in T_g with pressure is not assumed to have the same value of μ .

The mean-square displacements for the glass region ($T < T_g$) can then be related to values at T_g by

$$d^2(P, T) = d_g^2(P) \frac{T}{T_g(P)}, \quad (20)$$

where

$$d_g^2(P) = \begin{cases} d_0^2 \frac{T_g(P)}{T_0} \left[\exp(-\alpha_{P,0}(T_g(P) - T_0))(1 + \mu\kappa_{T,0}\Delta P)^{1/\mu} \right]^{(\frac{1}{3}-\mu)} & \nu = 0, \mu \neq 0 \\ d_0^2 \frac{T_g(P)}{T_0} \left[(1 - \nu\alpha_{P,0}(T_g(P) - T_0))^{1/\nu} (1 + \mu\kappa_{T,0}\Delta P)^{1/\mu} \right]^{(\frac{1}{3}-\mu)} & \nu \neq 0, \mu \neq 0 \end{cases}. \quad (21)$$

TABLE II. Fit of T_g to MD simulation data at low temperatures. In both cases, $\nu = 0$.

μ	Pressure dependence	Constant	Fit		$\chi^2 \times 10^5$
			value	Uncertainty	
0.70 ± 0.10	Constant	T_g (K)	192.8	2.2	2.21
	Linear	$T_{g,0}$ (K)	197.2	3.0	
	Logarithmic	c (K/MPa)	0.012	0.006	2.02
1	Logarithmic	$T_{g,0}$ (K)	199.9	3.1	1.78
		c	24.8	12.5	
	Constant	T_g (K)	193.3	2.3	2.33
1	Linear	$T_{g,0}$ (K)	197.7	3.1	2.14
		c (K/MPa)	0.012	0.006	
	Logarithmic	$T_{g,0}$ (K)	200.6	3.2	1.85
c	40.7	20.4			

The values of d_0^2 , $\alpha_{P,0}$, and $\kappa_{T,0}$ take on the values from the high temperature region so that T_g and c are the only unknowns.

In this section, the parameters in Eq. (21) take on the values for d_0^2 , $\alpha_{P,0}$, and $\kappa_{T,0}$ in Table I. Equations (20) and (21) using different assumptions for the pressure dependence of T_g [Eqs. (17)–(19)] are fit to data for 0 K < $T \leq 160$ K from the temperature data set (i.e., 0 K < $T \leq 320$ K at $P = 0.1, 300, 700$, and 1000 MPa) of the MD simulation data for HEWL to find values for $T_{g,0}$ and c . Results for $T_{g,0}$ and c for with error analysis are reported in Table II (further details for $\mu = 1$ and $\nu = 0$ in Table S5 of the [supplementary material](#) and for fitted μ and $\nu = 0$ in Table S6 of the [supplementary material](#)). First, $d^2(P, T)$ is fit assuming that T_g is invariant with respect to pressure [Eq. (17)]. When the calculated $d^2(P, T)$ is compared to the simulation data over the full range of temperatures [Fig. 2(a)], the temperature dependence over the entire temperature range is much improved and the predicted $T_{g,0} = 193$ K is near other results for proteins.^{10–12} Next, assuming that T_g varies linearly with pressure [Eq. (18)] or logarithmically with pressure [Eq. (19)], the calculated $d^2(P, T)$ is compared to the simulation data, the temperature dependence is also good over the entire temperature range [shown for Eq. (19) in Fig. 2(b)]. Although difficult to see, logarithmic dependence of T_g gives the best fit since the reduced χ^2 is $\sim 20\%$ smaller than the constant T_g . Although the uncertainty in the value of c is large since data for only four values of pressure were used, the variation in T_g over the pressure range studied here is fairly large, from 201 K at 0.1 MPa to 191 K at 1000 MPa for $\mu = 1$ and $\nu = 0$.

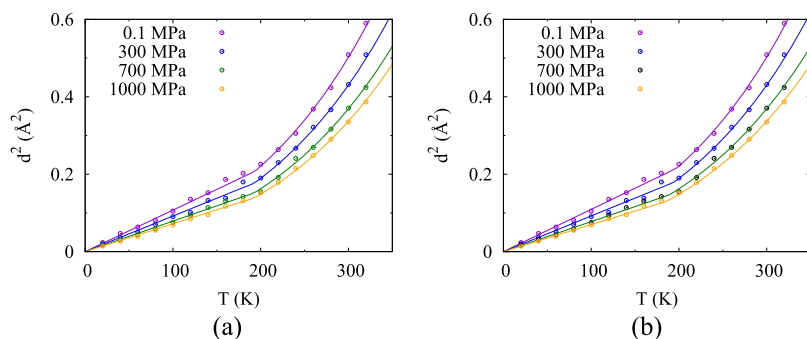


FIG. 2. Mean-square displacement $d^2(P, T)$ versus temperature T at various pressures calculated with $\mu = 0.7$ and $\nu = 0$ using parameters in Table I, which follow Eq. (16) above T_g and (a) Eqs. (17), (20), and (21) below T_g , which is independent of pressure, or (b) Eqs. (19)–(21) below T_g , which varies with pressure, compared to MD simulation data.

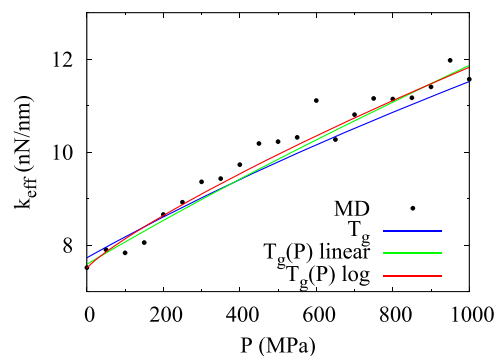


FIG. 3. Effective force constant k versus pressure calculated with $\mu = 0.7$ and $\nu = 0$ using parameters in Table I and either a pressure-independent T_g (blue line), the linearly pressure-dependent $T_g(P)$ (green line), or the logarithmically pressure-dependent $T_g(P)$ (red line), compared to MD simulation data for k (black dots).

C. The shape of the underlying potential

The effects of pressure on the shape of the underlying potential are also examined via an effective force constant k as a function of P . As in the work of Meinhold *et al.*,⁵ k are calculated from the displacements below T_g so that the underlying potential without the contributions of multiple conformational substates is being examined. Meinhold *et al.*⁵ calculated k using the following equation:

$$k(P) = \frac{6k_B}{(\partial \langle d^2 \rangle / \partial T)_P}, \quad (22)$$

where the MD data were fitted for the slope in the denominator. In addition, by substituting Eqs. (17) and (18), or (19) into Eq. (21), k can be calculated by

$$k(P) = \frac{6k_B T_g(P)}{d_g^2(P)}. \quad (23)$$

The effective force constant k calculated using Eq. (23) with parameters from Tables I and II can be compared to k from the MD simulation data. The calculated k assuming a pressure-dependent $T_g(P)$ predict the curvature seen in the simulation k better than those calculated assuming a pressure-independent T_g (Fig. 3). Interestingly, when k in Eq. (23) is fit directly to the simulation data for k (i.e., the black dots in Fig. 3), the fitted parameters for a pressure-independent T_g or pressure-dependent $T_g(P)$ (Tables S5 and S6 of the [supplementary material](#)) are similar to those determined by the fit to the temperature data set for d^2 described above. In addition, although the reduced χ^2 for fits to k are considerably higher than the

fits to d^2 , the fits to k from simulation for a pressure-dependent $T_g(P)$ are also better than a pressure-independent T_g , since the reduced χ^2 is $\sim 20\%$ smaller (Tables S5 and S6 of the [supplementary material](#)). Thus, a pressure-dependent $T_g(P)$ is better than a pressure-independent T_g for fitting both the extensive simulation data for d^2 as a function of temperature at only four pressures, and the extensive simulation data for k as a function of pressure.

IV. DISCUSSION

We begin with a discussion of how a quasiharmonic analysis can be used to interpret the physical origins of pressure and temperature effects on atomic fluctuations in proteins. The analysis is demonstrated on 1 ps mean-square displacements of protein hydrogen atoms only and not the surrounding solvent from 1 ns simulations of HEWL at different pressures and temperatures. Although the dynamics of heavy atoms are preferred, as pointed out in the Introduction, Meinhold *et al.*⁵ have shown that the dynamics of protein hydrogen atoms are a good measure of the dynamics of all protein atoms and thus the effective harmonic potential in which they move can be considered to be created by the protein environment. Thus, α_P and κ_T found from these simulations are intrinsic to the protein. In particular, these intrinsic quantities differ from the partial quantities of proteins in aqueous solutions because the latter also contains contributions from surface hydration. In addition, they are limited to a single conformational state since more motion (i.e., transitions to other conformational states) will occur on the μs and ms time scales. However, even at the time scales of these simulations, an increase in the dependence of the fluctuations on temperature over what can be attributed to phonon modes of a single substate occurs above ~ 200 K, which indicates that transitions to different substates occur. Thus, simulations on this time scale appear informative about dynamics of different substates within a conformational state, which are described in the quasiharmonic approximation via larger frequencies. Since the fluctuations are fit well assuming classical Einstein independent harmonic oscillators, these results indicate that the protein is not behaving like a true liquid above T_g but instead has a well-defined average structure reminiscent of a solid, consistent with the interpretation of the observed transition in proteins as a dynamical transition rather than a true glass-liquid transition.^{10–12} However, the oscillators are not truly non-interacting, which may be reflected in the best fit values of $\mu = 0.7$ and $\nu = 0$, while the ideal gas values are $\mu = 1$ and $\nu = -1$. In addition, since the assumptions that α_P is independent of P and κ_T is independent of T (see Sec. II) give good agreement with the simulation data, temperature and pressure effects appear to arise from different physical processes.

The isobaric thermal expansion coefficient α_P is a measure of the volume changes with temperature at constant pressure. Here, its physical origin is suggested by the dynamical transition temperature T_g found in the simulation data since T_g has been attributed in proteins to a minimum temperature where the thermal energy is sufficient to overcome activation energies to other substates. Thus, since the fitted value of α_P describes the temperature dependence of the simulation data

for the fluctuations above T_g , it can also be attributed to transitions to other substates. In particular, since α_P is positive, the fluctuations increase not only directly due to temperature but also due to expansion caused by accessing other substates, in which an atom moves in a harmonic energy well similar to that in the underlying potential but with a shifted mean position. In addition, over the small temperature range examined here, α_P appears independent of volume since $\nu = \sim 0$, and examination of a larger temperature range will be necessary to determine any volume dependence. However, the lack of dependence of α_P on volume and thus the separation between neighboring atoms further supports that the physical origin of α_P is mainly due to transitions between substates rather than in the effective energy wells of one substate.

The isothermal compressibility κ_T is a measure of the volume change with pressure at constant temperature. Here, κ_T was found to be almost directly proportional to the volume. More importantly, since the assumption that κ_T is the same above and below T_g (i.e., it is independent of the temperature) gives good agreement with the pressure dependence of the simulation data, pressure can be interpreted to have the same effect on the local minimum in the potential energy surface corresponding to a single substate below T_g as on the local minima associated with each substate above T_g , assuming the local minima of each substate are similar. In other words, κ_T describes the effects of pressure on the local minima in a given substate, regardless of which substate. In addition, since κ_T is positive, the effect of the increased pressure at this time scale is apparently to move the neighboring atoms closer, which narrows the effective energy well for a given atom and thus increases its k . However, at larger time scales, pressure has been noted to increase populations of other conformations in proteins.³⁰

The dependence of T_g on pressure is also informative. A decreasing T_g with pressure appears to fit the simulation data for both d^2 and k better than a constant T_g . This indicates that the barrier heights between substates are dependent on pressure in this simulation, in disagreement with Meinhold *et al.*,⁵ and in particular, pressure lowers the barriers. However, the scatter in values of d^2 in the simulation data and large uncertainty in c (due in part to having d^2 for only four pressures) make the pressure-dependence of T_g somewhat questionable. In addition, another subtle factor is that the heating and pressurizing in the HEWL data were for 100 ps and 600 ps, respectively, for each P - T value, and so slight relaxation due to pressure from the crystal structure may occur. In relation to this, simulations of dihydrofolate reductase (DHFR), which were heated and pressurized for 60 ps each using the Nosé-Hoover^{25,26} algorithm implemented in CHARMM,³¹ actually have the opposite sign for c (Huang, Rodgers, Hemley, and Ichiye, unpublished results). However, when the starting structure was equilibrated at a higher pressure (i.e., 220 atm), T_g was lower. Thus, both studies indicate that the barrier to collective motions may be decreased by high pressure, but whether it is apparent in the pressure dependence of T_g from P - T simulations starting from a single structure equilibrated at one pressure or if the pressure dependence of $T_{g,0}$ from P - T simulations starting from several structures equilibrated at different pressures may depend on the extent to

which the simulation at a given P - T is allowed to relax to the pressure.

Regardless, the nonlinear increase with pressure of the force constant for the underlying potential energy minimum below T_g observed in the HEWL simulation data appears to be due to a combination of the pressure-dependent force constant of the underlying potential and the decrease in T_g with increasing pressure rather than a pressure-induced transition as suggested by Meinhold *et al.*⁵ While the pressure-dependence of T_g is described here by Eqs. (18) and (19), the exact dependency on pressure is not clear, and the fitted values of c should not be over-interpreted, given the large uncertainty due to being fit to data for only four pressures. In addition, the physical origins of the pressure dependence of T_g are likely not the same as those for κ_T and instead may be due to pressure affecting the separation of the substates from each other, whether mechanically or thermodynamically. If this also occurs for transitions between conformational states, the analysis presented here could help explain pressure-induced unfolding.

Finally, at longer time scales than examined here, motions occur that are better described as transitions to different conformational states. Since pressure, in addition to temperature, is known to affect populations of conformational states,³⁰ α_P and κ_T are likely to be affected. The dynamics of heavy atoms from simulations on longer timescales that explore the free energy surface or simulations that explore more of the potential energy surface by starting from proteins equilibrated at different pressures may be more informative about problems involving transitions to other conformational states, such as protein unfolding. In particular, results from simulations on a ~ 50 ns time scale are intriguing since the fluctuations actually increase with pressure.³²

V. CONCLUSIONS

Atomic fluctuations are important for the structure and function of proteins and can be determined experimentally from X-ray and neutron studies or calculated from molecular dynamics simulations. Here, a method for analyzing atomic fluctuations is developed in which the effective potential energy well for an atom is described as quasiharmonic so that volume changes due to temperature and pressure are separated in terms of an intrinsic α_P and κ_T for the protein. The applicability of this quasiharmonic analysis is demonstrated on data from a previous molecular dynamics simulation of HEWL by Meinhold *et al.*⁵ In particular, the pressure and temperature dependence of the picosecond mean-square displacements of the HEWL simulations is shown here to be described by a quasiharmonic approximation with a constant α_P and a volume dependent κ_T above T_g . Below T_g , the calculated displacements agree with the simulation data assuming that the temperature dependence is frozen at its T_g value but that the pressure dependence is the same as in the liquid region. Finally, the nonlinear pressure dependence of k appears to be due to the changes in T_g and frequencies with pressure rather than a transition in behavior. A quasiharmonic analysis can thus lead to a better understanding of the energy landscapes of complex biomolecules. Indeed, quasiharmonic analyses of atomic fluctuations from longer time scale

simulations, especially if the solvent is also analyzed, could be useful in understanding problems such as protein folding.

SUPPLEMENTARY MATERIAL

See [supplementary material](#) for more information on the simulation methods of Meinhold *et al.*,⁵ for tables of fits of mean-square displacements with different assumptions for fitting μ and ν , and for figure of mean-square displacements versus temperature assuming no glass transition.

ACKNOWLEDGMENTS

T.I. is grateful for support from a grant from the National Institutes of Health No. R01 GM122441 and for support from the McGowan Foundation. J.M.R. and R.J.H. acknowledge support from the Department of Energy/National Nuclear Security Administration through Grant No. DE-NA-0002006 for the Carnegie/DOE Alliance Center (CDAC) and from the Alfred P. Sloan Foundation through the Deep Carbon Observatory. The views and conclusions contained in this document are those of the authors and should not be interpreted as necessarily representing the official policies or endorsements, either expressed or implied, of the U.S. Government. This work used computer time on the Extreme Science and Engineering Discovery Environment (XSEDE) granted via No. MCB990010, which is supported by the National Science Foundation Grant No. OCI-1053575 and the Medusa cluster, which is maintained by the University Information Services at Georgetown University.

- ¹H. Frauenfelder and D. T. Leeson, *Nat. Struct. Biol.* **5**, 757 (1998).
- ²J. N. Onuchic and P. G. Wolynes, *Curr. Opin. Struct. Biol.* **14**, 70 (2004).
- ³F. G. Parak, *Rep. Prog. Phys.* **66**, 103 (2003).
- ⁴L. Meinhold and J. C. Smith, *Phys. Rev. E* **72**, 061908 (2005).
- ⁵L. Meinhold, J. C. Smith, A. Kitao, and A. H. Zewail, *Proc. Natl. Acad. Sci. U. S. A.* **104**, 17261 (2007).
- ⁶H. M. Berman, J. Westbrook, Z. Feng, G. Gilliland, T. N. Bhat, H. Weissig, I. N. Shindyalov, and P. E. Bourne, *Nucleic Acids Res.* **28**, 235 (2000).
- ⁷T. Ichiye and M. Karplus, *Proteins: Struct., Funct., Genet.* **2**, 236 (1987).
- ⁸T. Ichiye and M. Karplus, *Biochemistry* **27**, 3487 (1988).
- ⁹T. Ichiye and M. Karplus, *Proteins: Struct., Funct., Genet.* **11**, 205 (1991).
- ¹⁰D. Vitkup, D. Ringe, G. A. Petsko, and M. Karplus, *Nat. Struct. Biol.* **7**, 34 (2000).
- ¹¹H. Frauenfelder, *Phys. E* **42**, 662 (2010).
- ¹²D. Ringe and G. A. Petsko, *Biophys. Chem.* **105**, 667 (2003).
- ¹³P. Gillet, R. J. Hemley, and P. F. McMillan, in *Ultrahigh-Pressure Mineralogy: Physics and Chemistry of the Earth's Deep Interior*, edited by R. J. Hemley (Mineralogical Society of America, Washington, DC, 1998), Vol. 37, p. 525.
- ¹⁴B. Fultz, *Prog. Mater. Sci.* **55**, 247 (2010).
- ¹⁵D. C. Wallace, *Thermodynamics of Crystals*, 1st ed. (John Wiley and Sons, New York, 1972).
- ¹⁶W. Doster, S. Cusack, and W. Petry, *Nature* **337**, 754 (1989).
- ¹⁷P. W. Fenimore, H. Frauenfelder, B. H. McMahon, and F. G. Parak, *Proc. Natl. Acad. Sci. U. S. A.* **99**, 16047 (2002).
- ¹⁸D. P. Nash and J. Jonas, *Biochemistry* **36**, 14375 (1997).
- ¹⁹D. Harrison and E. A. Moelwyn-Hughes, *Proc. R. Soc. London, A* **239**, 230 (1957).
- ²⁰D. P. Kharakoz, *Biophys. J.* **79**, 511 (2000).
- ²¹H. J. C. Berendsen, D. van der Spoel, and R. van Drunen, *Comput. Phys. Commun.* **91**, 43 (1995).
- ²²E. Lindahl, B. Hess, and D. van der Spoel, *J. Mol. Model.* **7**, 306 (2001).
- ²³G. A. Kaminski, R. A. Friesner, J. Tirado-Rives, and W. L. Jorgensen, *J. Phys. Chem. B* **105**, 6474 (2001).

- ²⁴M. Refaee, T. Tezuka, K. Akasaka, and M. P. Williamson, *J. Mol. Biol.* **327**, 857 (2003).
- ²⁵S. Nosé, *J. Chem. Phys.* **81**, 511 (1984).
- ²⁶W. G. Hoover, *Phys. Rev. A* **31**, 1695 (1985).
- ²⁷M. Parrinello and A. Rahman, *J. Appl. Phys.* **52**, 7182 (1981).
- ²⁸S. Nosé and M. L. Klein, *Mol. Phys.* **50**, 1055 (1983).
- ²⁹R. J. Hemley, A. P. Jephcoat, H. K. Mao, L. C. Ming, and M. H. Manghnani, *Nature* **334**, 52 (1988).
- ³⁰K. Akasaka, *Chem. Rev.* **106**, 1814 (2006).
- ³¹B. R. Brooks, C. L. Brooks III, A. D. MacKerell, Jr., L. Nilsson, R. J. Petrella, B. Roux, Y. Won, G. Archontis, C. Bartels, S. Boresch, A. Caffisch, L. Caves, Q. Cui, A. R. Dinner, M. Feig, S. Fischer, J. Gao, M. Hodoscek, W. Im, K. Kuczera, T. Lazaridis, J. Ma, V. Ovchinnikov, E. Paci, R. W. Pastor, C. B. Post, J. Z. Pu, M. Schaefer, B. Tidor, R. M. Venable, H. L. Woodcock, X. Wu, W. Yang, D. M. York, and M. Karplus, *J. Comput. Chem.* **30**, 1545 (2009).
- ³²Q. Huang, J. M. Rodgers, R. J. Hemley, and T. Ichiye, *J. Comput. Chem.* **38**, 1174 (2017).